OH 1.563 μm ABSORPTION FROM STARSPOTS ON ACTIVE STARS

DOUGLAS O'NEAL[1] AND JAMES E. NEFF

Department of Astronomy and Astrophysics, The Pennsylvania State University, 525 Davey Laboratory, University Park, Pennsylvania 16802

Electronic mail: oneal@astro.psu.edu

Received 1996 September 4; revised 1996 November 21

ABSTRACT

We present results from a study of starspots on active stars using a pair of vibrational-rotational absorption lines of the OH molecule near 1.563 μm. We detect excess OH absorption due to dark, cool starspots on the RS CVn binaries II Pegasi, V1762 Cygni, and λ Andromedae. This is the first detection of OH absorption from spots on stars other than the Sun. We have measured absorption equivalent widths of these OH lines (which are blended at the resolution of our observations) in inactive giant and dwarf stars of spectral types G, K, and M. We find that the total equivalent width of the line pair increases approximately linearly as effective temperature decreases from 5000 K to 3000 K. This greatly extends the temperature range over which starspots can be detected through molecular absorption features. We measure starspot filling factors by fitting the spectra of active stars with linear combinations of comparison star spectra representing the spot and non-spot regions of the star. Fitting only one spectral feature, we cannot derive independent constraints on starspot area and temperature. Assuming spot temperatures based on previous analyses, we find (for one epoch) spot filling factors between 35% and 48% for II Peg, 22% and 26% for λ And, and 27% and 32% for V1762 Cyg.
[S0004-6256(97)00503-7]

1. INTRODUCTION

In previous papers (Neff *et al.* 1995, hereafter Paper I; and O'Neal *et al.* 1996, hereafter Paper II) we develop a spectroscopic technique to measure the temperatures and filling factors of starspots on magnetically active stars. In that technique, we primarily use the absorption bands of the TiO molecule at 7055 Å and 8860 Å, using spectra of inactive M stars to model the spotted regions of the active star photospheres and spectra of inactive G and K stars to model the non-spotted regions, and combining these spectra to fit the TiO bands observed from active stars.

Traditionally, photometric light-curve modeling has been used to measure properties of starspots (e.g., Strassmeier *et al.* 1994; Henry *et al.* 1995). That technique has the disadvantage that it can only measure an asymmetric spot distribution or differences from a presumed "immaculate" light-level; a longitudinally-symmetric distribution will produce no variation of the star's brightness. More spatial detail can be derived using Doppler imaging (e.g., Vogt *et al.* 1987; Piskunov *et al.* 1990; Kürster 1993), in which asymmetries in a line profile from a rapidly-rotating star are used to model the asymmetries on the stellar surface. The advantage of our spectroscopic technique is that it can detect starspots even on a slowly-rotating star and without regard to their spatial distribution.

The TiO bands, while very useful for independently constraining starspot area and temperature, can only be observed for spot temperatures $T_S \lesssim 4000$ K. Thus, to extend the temperature range over which starspots can be observed spectroscopically, we searched for temperature-dependent features detectable at higher temperatures. Also, in the visible starspots are much fainter than the non-spotted photosphere of active stars, thus they only weakly affect the overall spectrum of the star. For this reason, we searched for spectral features in the near-infrared, where the spots become brighter relative to the unspotted photosphere.

We considered using the first-overtone bands of CO near 2.2 μm. However, these bands are detectable in stars as warm as 8000 K (Lançon & Rocca-Volmerange 1992), so contributions to the overall CO band strength of active star spectra from the non-spot and spotted photosphere might not be easily separable. In addition, for $T_{\rm eff} < 3800$ K, the CO absorption features are blended with bands of H_2O (Lançon & Rocca-Volmerange 1992; Terndrup *et al.* 1991). Finally, the CO bands are formed at a wide range of heights in a stellar atmosphere (e.g., Ayres & Testerman 1981).

We next considered observing atomic lines. Compiling a list of candidate lines from sources such as Tinney *et al.* (1993), Lançon & Rocca-Volmerange (1992), and Kleinmann & Hall (1986), we examined all these features in both the solar photosphere and in sunspots, using the infrared solar spectral atlases by Wallace & Livingston (1991, 1992). A set of five Ti I lines between 2.18 and 2.23 μm were the only features whose strengths differ sufficiently between a sunspot and the non-spotted solar photosphere to be potentially useful as spot diagnostics on active stars. However, these lines are quite magnetically sensitive. For optically thick

[1]Visiting Astronomer, Kitt Peak National Observatory, National Optical Astronomy Observatories, operated by AURA, Inc., under cooperative agreement with the National Science Foundation.

 0004-6256/97/113(3)/1129/9/$10.00

lines, Zeeman splitting (even if unresolved) will increase a line's equivalent width due to redistribution of opacity out of the line core (Leroy 1962; Basri & Marcy 1994). Thus, magnetic sensitivity would enhance the strengths of the lines in starspots and lead us to overestimate the spot filling factor f_S.

We then considered using infrared absorption lines of OH to observe starspots. These lines are very sensitive to temperature (Grevesse *et al.* 1984); they are quite strong in sunspots and in the spectrum of Arcturus (Hinkle *et al.* 1995), but are invisible in the solar photosphere (Wallace & Livingston 1992). We chose to observe the 6397 cm^{-1}, 3–1 P2e and P2f (J=5.5) transitions because they lie in a relatively uncrowded region of the H-band spectrum. Also, there is no skyglow or atmospheric absorption line at this wavelength (Hinkle *et al.* 1995). These features are detectable at temperatures several hundred degrees higher than the 4000 K at which TiO bands are too weak to be seen from starspots on active stars. We also gain by moving to the H-band because of the greater relative brightness of starspots relative to the star's photosphere. For example, in a star with T_S = 3500 K and non-spot temperature T_Q = 5000 K, the ratio of continuum surface flux between the spot and photosphere, R_λ, is 0.11 at the 7050 Å (based on models by Kurucz 1992) and 0.21 at 8850 Å, but it is 0.49 at 1.56 μm.

The three magnetically active stars discussed in this paper are spectroscopic binaries; the secondary stars of II Peg and λ And have never been detected, while the secondary of V1762 Cyg was only recently detected (Osten & Saar 1997). We calculate (see Sec. *3.1*), however, that plausible companion stars would be sufficiently faint in the H band, relative to their primaries, that any OH absorption strength arising in the secondary would represent only a negligible level of contamination and does not affect our analysis.

2. OBSERVATIONS AND ANALYSIS

The data were obtained from 1996 June 13–18 with the Coudé Feed Telescope at Kitt Peak National Observatory using the NICMASS infrared camera. The NICMASS uses a 256 × 256 HgCdTe NICMOS3 array and is installed at the Camera 5 focus at the Coudé Feed. Using the NICMASS with an echelle grating yields a 2-pixel resolution $\lambda/\Delta\lambda \approx 42{,}000$. The high spectral orders observed with the echelle grating require narrowband filters for order separation. In the absence of a narrowband filter designed to be used cooled at 1.563 μm, we used a Spectragon filter with a central wavelength (measured when warm) of 1.567 μm and a bandpass of 0.03 μm. Cooling this filter would have shifted its bandpass enough so that it would have no longer transmitted the wavelengths we wished to observe. Therefore, this filter was used warm and affixed to the outside of the dewar window, and a broadband H-band filter was placed in the NICMASS dewar for thermal blocking. This arrangement yielded a higher background level than if it had been possible to cool the narrowband filter, so we were restricted to exposures of 15 minutes or less to avoid saturating the detector with background emission. In practice, our longest exposures, of II Peg and V1762 Cyg, were 12 minutes long.

TABLE 1. Properties of active stars.

	V1762 Cyg	λ And	II Peg
HD	179094	222107	224085
Spectral Type	K1 III-IV	G8 III-IV	K2-3 IV
P_{rot}	28.5895[a]	53.95[b]	6.72422[c]
HJD for $\phi = 0$	2,442,479.214[a]	2,443,829.2[b]	2,443,033.47[c]
log g	3.2	2.5	3.7
T_Q	4550 K	4750 K[d]	4800 K
T_S	3450 K	3650 K	3500 K

[a]Strassmeier *et al.* (1994).
[b]Boyd *et al.* (1983).
[c]Vogt (1981).
[d]Donati *et al.* (1995).

Our spectra were centered on the OH lines at 1.563 μm (6397 cm^{-1}), and covered a 45 Å bandpass with 0.173 Å per pixel. A Th-Ar source yielded no emission lines in our bandpass, so wavelength calibration was done by taking spectra of Arcturus and using the scale in the Arcturus Atlas (Hinkle *et al.* 1995). Bias and background subtraction was accomplished by taking two consecutive spectra of each target star with the same exposure time but illuminating different rows of the detector. When this was done, the rows containing the spectrum in the first exposure contained pure background in the second exposure, and vice-versa. Subtracting the two exposures left behind two background-free spectra of the star. After flat-field division, these two spectra were extracted and added together. In some cases, we took multiple pairs of spectra of our fainter target and comparison stars, then after adding together the two components of each pair, combined those spectra to yield a higher S/N and to produce one final, resultant spectrum of the star for that night. The resultant spectra of our bright comparison stars and λ And have S/N ≈ 200 per pixel, our spectra of V1762 Cyg have S/N ≈100, and the spectra of II Peg, with exposure times limited due to background emission, have S/N ≈ 50. In practice, we achieved a resolution of 3.2 pixels, as judged from telluric lines in the spectrum of a hot star, corresponding to a broadening velocity of 11 km s^{-1}. The effective resolution was therefore $\lambda/\Delta\lambda \approx 26{,}000$.

In Table 1 we list the properties of the three active stars observed for this program. Except where noted otherwise, T_Q and T_S are based on measurements reported in Paper II, and the sources for the ephemerides are given in the footnotes. Table 2 is a log of our observations of these three stars. Each line in this table refers to a consecutive pair of exposures, which were then subtracted to remove background.

We also observed a set of inactive comparison stars covering the range of spot and non-spot temperatures expected for the active stars. These comparison stars are listed in Table 3. Photometry for the stars comes from Stauffer & Hartmann (1986) and the Bright Star Catalog (Hoffleit & Jaschek 1982). In cases where no H-band photometry was available, we estimated an H magnitude from the V magnitude and the star's spectral type by interpolating between $V-H$ colors of standard stars listed by Wamstecker (1981)

TABLE 2. Log of observations of active stars.

Star	HD	Date	JD (mid)	Phase (mid)
V1762 Cyg	179094	1996 June 14	2,450,248.88	0.77
		1996 June 15	2,450,249.83	0.80
		1996 June 15	2,450,249.84	0.80
		1996 June 16	2,450,250.81	0.83
		1996 June 16	2,450,250.83	0.83
		1996 June 17	2,450,251.82	0.87
		1996 June 17	2,450,251.83	0.87
		1996 June 17	2,450,251.85	0.87
		1996 June 18	2,450,252.81	0.90
		1996 June 18	2,450,252.83	0.90
		1996 June 18	2,450,252.84	0.91
λ And	222107	1996 June 15	2,450,249.92	0.01
		1996 June 16	2,450,250.90	0.03
		1996 June 17	2,450,251.90	0.05
		1996 June 18	2,450,252.89	0.07
II Peg	224085	1995 June 15	2,450,249.89	0.20
		1995 June 15	2,450,249.91	0.20
		1995 June 15	2,450,249.93	0.20
		1995 June 15	2,450,249.95	0.21
		1995 June 16	2,450,250.86	0.34
		1996 June 16	2,450,250.88	0.35
		1996 June 16	2,450,250.92	0.35
		1996 June 16	2,450,250.93	0.35
		1996 June 17	2,450,251.87	0.49
		1996 June 17	2,450,251.88	0.49
		1996 June 17	2,450,251.91	0.50
		1996 June 17	2,450,251.93	0.50
		1996 June 18	2,450,252.86	0.64
		1996 June 18	2,450,252.88	0.64
		1996 June 18	2,450,252.90	0.65
		1996 June 18	2,450,252.92	0.65

TABLE 3. Properties of comparison stars.

HD	HR	Name	Spectral Type	V	H	$(B-V)$	$(R-I)$	$T_{\rm eff}$
			A. Giant Comparison Stars					
196755	7896	κ Del	G2 IV	5.0	3.4	0.72	...	5550
126868	5409	φ Vir	G2 IV	4.8	3.2	0.70	0.37	5525
141714	5889	δ CrB	G3.5 III-IV	4.6	2.7	0.80	0.42	5200
198149	7957	η Cep	K0 IV	3.4	0.9	0.92	0.49	4925
135722	5681	δ Boo	G8 III	3.5	1.4	0.95	0.51	4900
145001	6008	κ Her	G8 III	5.0	3.0	0.95	0.46	4900
194013	7794		G8 III-IV	5.3	3.3	0.97	0.50	4850
109317	4783		K0 III	5.4	2.9	1.00	0.50	4800
142091	5901	κ CrB	K1 IV	4.8	2.3	1.00	0.49	4800
145328	6018	τ CrB	K1 III-IV	4.8	2.3	1.01	0.54	4775
95345	4291	58 Leo	K1 III	4.8	2.3	1.16	0.56	4600
110014	4813	χ Vir	K2 III	4.7	2.1	1.23	0.61	4350
124897	5340	α Boo	K1.5 III	−0.0	−2.8	1.23	0.65	4350
127665	5429	ρ Boo	K3 III	3.6	0.8	1.30	0.65	4300
116870	5064	68 Vir	M0 III	5.3	1.8	1.52	0.87	3950
164058	6705	γ Dra	K5 III	2.2	−0.8	1.52	0.85	3950
141477	5879	κ Ser	M0.5 III	4.1	0.4	1.62	0.98	3775
119149	5150	82 Vir	M1.5 III	5.0	1.0	1.63	1.16	3700
183630	7414	36 Aql	M1 III	5.0	1.4	1.75	...	3700
112300	4910	δ Vir	M3 III	3.4	−1.0	1.58	1.33	3650
133216	5603	σ Lib	M3 III	3.3	−0.7	1.70	1.29	3650
102620	4532	II Hya	M4 III	5.1	0.8	1.60	...	3550
123657	5299	BY Boo	M4.5 III	5.3	−0.1	1.59	1.66	3550
113866	4949	FS Com	M5 III	5.6	1.1	1.59	1.81	3475
175865	7157	R Lyr	M5 III	4.0	−0.5	1.59	1.91	3425
94705	4267	VY Leo	M5.5 III	5.8	−0.44	1.45	2.09	3325
117287	5080	R Hya	M7 III	5.0	−1.5	1.60	2.42	3050
			B. Dwarf Comparison Stars					
117176	5072	70 Vir	G4 V	5.0	3.3	0.71	0.39	5600
115617	5019	61 Vir	G6 V	4.7	2.8	0.71	0.36	5575
160346		Gl 688	K3 V	6.5	3.7	0.96	0.50	4850
111631		Gl 488	M0.5 V	8.5	5.1	1.40	0.66	3700
95735		Gl 411	M2 V	7.5	3.6	1.51	0.92	3350

and of other comparison stars with measured H magnitudes. $T_{\rm eff}$ values were computed using the methods described in Paper 2 and were rounded to the nearest interval of 25 K.

In Fig. 1 we present spectra of all our giant and subgiant comparison stars, with the 1.563 μm OH lines identified with an arrow. Other lines are identified in Hinkle *et al.* (1995). We removed the effects of the stars' differing heliocentric and radial velocities and plotted them all on the wavelength scale of the Arcturus Atlas. One can immediately see the increase in the strengths of the OH lines with decreasing $T_{\rm eff}$. We measured the combined equivalent width of the two OH lines for each comparison star (Fig. 2). The best linear fit to these equivalent widths is $EW = -0.486t + 2.375$ Å, where $t = T_{\rm eff}/1000$ K. This fit has an rms residual of 0.051 Å. The best second-order fit, $EW = 0.1597t^2 - 1.802t + 5.030$ Å, has an rms residual of 0.029 Å.

Figure 3 presents spectra of the smaller number of dwarf comparison stars we observed. From this limited set of dwarf stars, it appears that the OH lines are substantially weaker than in giant stars of the same temperature. The same behavior was observed for the absorption bands of TiO (Paper I). In Paper I we found that the TiO absorption from starspots on subgiant and giant active stars cannot be modeled using M dwarf spot comparison stars. In Paper II we discuss possible reasons for this. Qualitatively, the pressure balance inside starspots might be affected by the presence of a strong magnetic fields; this might reduce the gas pressure and mimic a lower gravity environment. In Papers I and II, we found that using M giants to model the TiO bands from spots on subgiant active stars can underestimate f_S by 5%–10%.

3. RESULTS

The monotonic increase in the strength of the OH absorption lines with decreasing $T_{\rm eff}$ confirms that these features can be a useful diagnostic of starspot properties. Since OH absorption is seen in stars as warm as 5000 K and since all three of our active target stars have T_Q cooler than this, both the non-spot and spotted regions of the photospheres of these stars contribute to the total OH absorption strength. In addition, at the 23 km s^{-1} rotation velocity of II Peg, the OH lines are blended with nearby weak lines. Nonetheless, excess absorption in the OH lines due to starspots is readily apparent in all our active star spectra. In Fig. 4 we have plotted the spectra of the II Peg, V1762 Cyg, and λ And, comparing them to rotationally-broadened spectra of standard stars with similar spectral type and $T_{\rm eff}$. The spectra are standardized in wavelength to remove the effects of differing radial and heliocentric velocities and binary orbital motions.

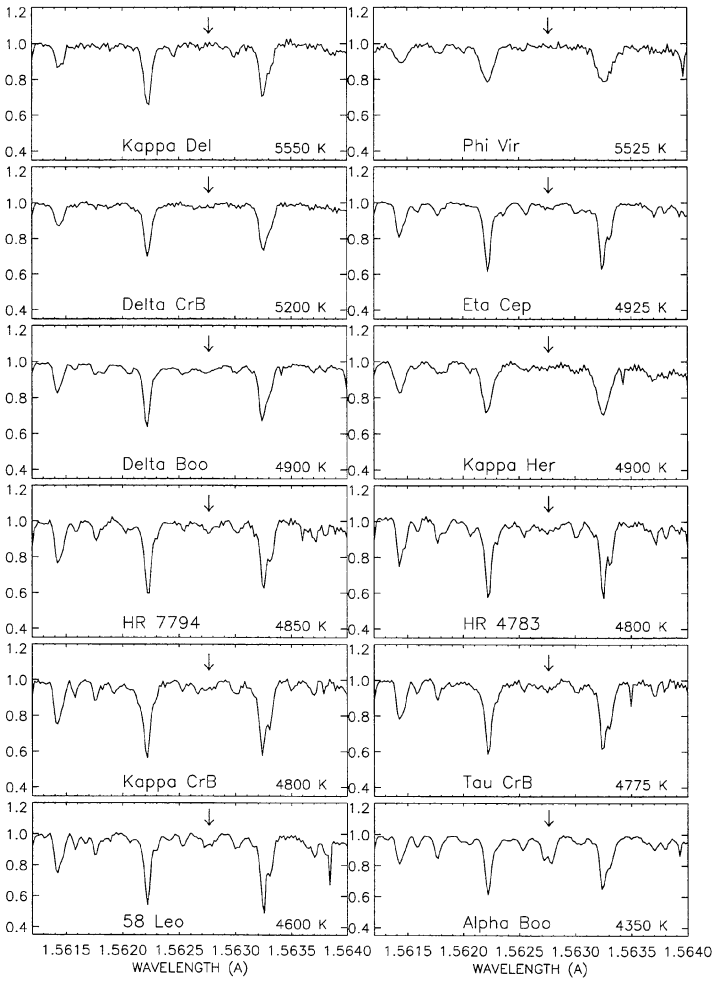

FIG. 1. 1.563 μm spectra of all 27 giant and subgiant comparison stars observed for this program. The position of the OH absorption lines is marked by an arrow; the feature is first visible around $T_{\rm eff}$ = 5000 K and increases in strength with decreasing $T_{\rm eff}$.

To quantify this excess OH absorption, we fit the spectra of the active stars using the STARMOD spectral synthesis code. STARMOD, written (Barden 1985) and later modified (by D. P. Huenemoerder and A. D. Welty) at Penn State, fits an observed spectrum with a linear combination of up to three model spectra. It has been used extensively (e.g., Welty & Wade 1995) to determine radial and rotational velocities and spectral types of systems of interest, and to find the relative brightnesses of stars in systems of two or three components. Given a target star spectrum to be fit, STARMOD constructs a model by shifting the standard star spectra in radial velocity and by applying a standard rotational broadening function (e.g., Gray 1988) with a limb-darkening coefficient ϵ = 0.6. The user inputs initial estimates for the radial velocity, $v \sin i$, and relative weight of each standard spectrum. These are iterated in succession until the best fit is achieved. In our case, the radial velocity and $v \sin i$ were fixed; before running the program, we shifted all spectra to a common wavelength scale and set $v \sin i$ to the best literature value for the active star being fitted.

In this study, we use the STARMOD routine to model each active star spectrum as a sum of two comparison star spectra: the G/K "non-spot" comparison star with $T_{\rm eff} = T_{\rm Q}$ and the M "spot" comparison star with $T_{\rm eff} = T_{\rm S}$. We restricted the fit to the wavelength region 1.5612 μm $\leq \lambda \leq$ 1.5640 μm. The best-fit relative weights of the two standard star spectra computed by STARMOD are directly related to the starspot filling factor on the active star. The normalized spectrum of the active star, $F_{\rm total}$, can be written as

$$F_{\rm total} = \frac{f_{\rm S} R_\lambda F_{\rm S} + (1 - f_{\rm S}) F_{\rm Q}}{f_{\rm S} R_\lambda + (1 - f_{\rm S})}, \quad (1)$$

where $f_{\rm S}$ is the spot filling factor, the total fractional projected area of spots on the observed hemisphere weighted by limb-darkening; R_λ is the continuum surface flux ratio between the spot and non-spot photosphere; and $F_{\rm S}$ and $F_{\rm Q}$ are the normalized spot and non-spot comparison spectra, respectively. STARMOD calculates the best relative weights, $W_{\rm S}$ and $W_{\rm Q}$, of the two comparison spectra, such that $F_{\rm total} = W_{\rm S} F_{\rm S} + W_{\rm Q} F_{\rm Q}$.

Therefore,

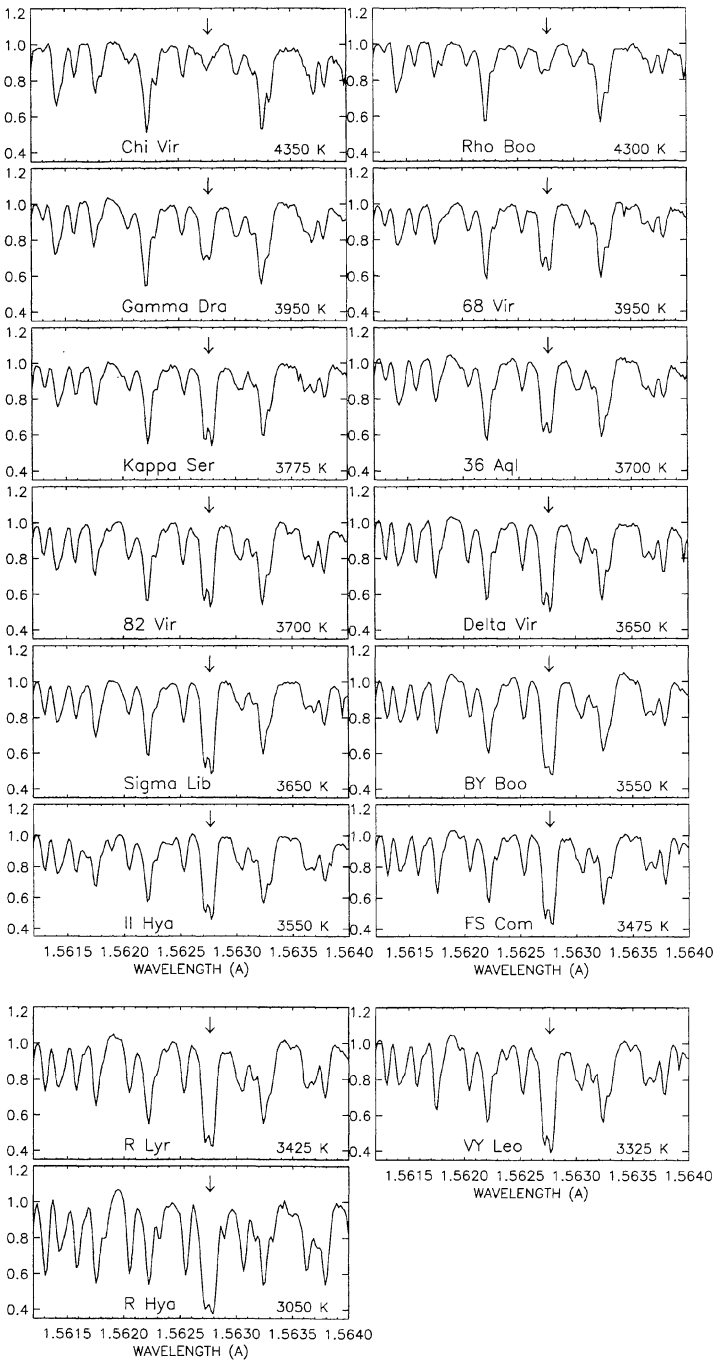

FIG. 1. (continued)

$$W_Q = \frac{1 - f_S}{(f_S R_\lambda) + (1 - f_S)} \quad (2)$$

and

$$W_S = \frac{f_S R_\lambda}{(f_S R_\lambda) + (1 - f_S)}, \quad (3)$$

so

$$f_S = \left(\frac{R_\lambda}{W_S} - R_\lambda + 1 \right)^{-1}. \quad (4)$$

The Kurucz (1992) models were used to compute R_λ.

We first created an array of spot standards and an array of non-spot standards. For each active star, the non-spot comparison array spans a $T_{\rm eff}$ range of $\approx T_Q \pm 300$ K. For II Peg and V1762 Cyg, in Paper 2 we measured $T_S = 3500$ K and 3450 K, respectively; O'Neal (1997) measured $T_S = 3650$ K

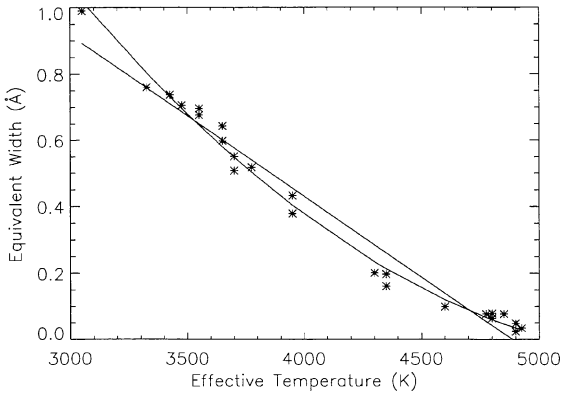

FIG. 2. Relation between equivalent width of the OH 1.563 μm feature and $T_{\rm eff}$ for giant and subgiant comparison stars. Equivalent width increases approximately linearly with decreasing $T_{\rm eff}$ from 5000 K to 3000 K. The measured values are plotted as asterisks, and the best first- and second-order fits to the $T_{\rm eff}$ vs EW relation are overplotted.

for λ And. To investigate what happens when various spot comparison stars are used to fit active star spectra, we used a spot comparison array spanning 3050 K$\leqslant T_{\rm S}\leqslant$ 3950 K for all three active stars. For each active star spectrum, we then used STARMOD to find the best-fit $f_{\rm S}$ using each spot/non-spot comparison star pair.

3.1 II Pegasi = HD 224085

II Peg is an extremely active single-lined, spectroscopic binary system with a spectral type K2–3 IV-V and $v \sin i$ =23 km s^{-1}. It exhibits V-band variations of up to 0.6 magnitude (e.g., Byrne *et al.* 1995; Doyle *et al.* 1988) and strong radio (Drake *et al.* 1989) and x-ray (Dempsey *et al.* 1993) activity. Using TiO bands, we have detected $f_{\rm S}$ as high as 56% (Paper 2), finding $T_{\rm Q}$ = 4800 K and $T_{\rm S}$ = 3500±100 K.

We obtained four pairs of spectra of II Peg on each of four consecutive nights, 1996 June 15–18. For each night, the eight spectra were added together to produce the final, normalized spectra plotted in Fig. 4. The four nights of observation span 45% of II Peg's 6.7 d rotational period.

We present in Fig. 5(a) the best-fit of the II Peg spectrum of June 18 computed using a non-spot comparison star of $T_{\rm Q}$ = 4800 K and a spot comparison star of $T_{\rm S}$ = 3550 K. No M giant having $T_{\rm eff}$ = 3500 K, the spot temperature computed for II Peg in Paper 2, was observed. This fit has $f_{\rm S}$ = 0.48 and an rms residual of 0.037; the relatively low S/N of the II Peg spectrum is the major contributor to this residual.

In Table 4 we list the spot filling factors for each active star observation. Using STARMOD, we fitted each active star spectrum using 4–6 spot comparison stars with temperatures within the active star's $T_{\rm S}$ error bars. We used a similar number of non-spot comparison stars having temperatures near the presumed $T_{\rm Q}$ value of the active star. We then interpolated among the $f_{\rm S}$ values computed for all these fits, and the results are given in Table 4 for each active star observation. For II Peg, the $f_{\rm S}$ values were interpolated for $T_{\rm S}$ = 3500 K and are not substantially different from the $f_{\rm S}$ values we found using TiO bands (Paper II). The quoted uncertainties primarily reflect the different $f_{\rm S}$ values calculated when different non-spot standard stars are used for the fits. These uncertainties result from the difficulty of perfectly normalizing the comparison star spectra and from intrinsic variations in the strength of OH absorption in comparison star spectra at a given $T_{\rm eff}$. For II Peg, the $T_{\rm S}$ error bars do not substantially contribute to the uncertainty in $f_{\rm S}$. In this $T_{\rm S}$ regime, the increasing strength of the intrinsic OH absorption from cooler starspots just compensates for the de-

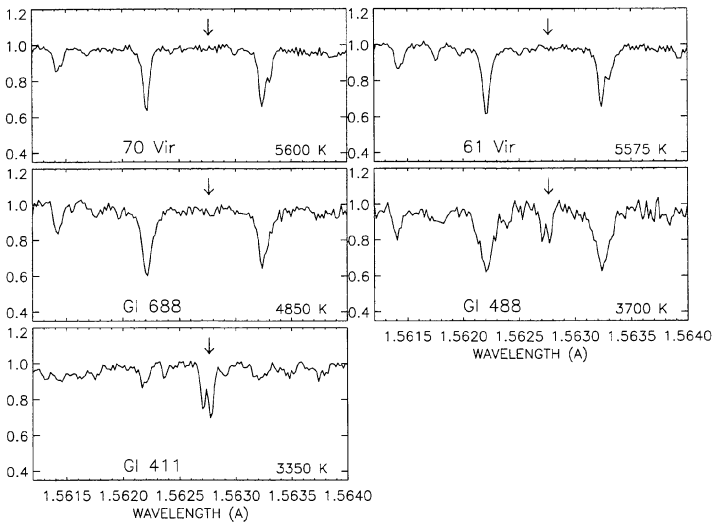

FIG. 3. 1.563 μm spectra of the 5 dwarf comparison stars observed for this program. The position of the OH absorption lines is marked by an arrow. Based on these limited data, the behavior of the OH feature with $T_{\rm eff}$ is similar for dwarfs as for giants of spectral types G and K, but the feature is weaker in M dwarfs than in M giants of the same $T_{\rm eff}$.

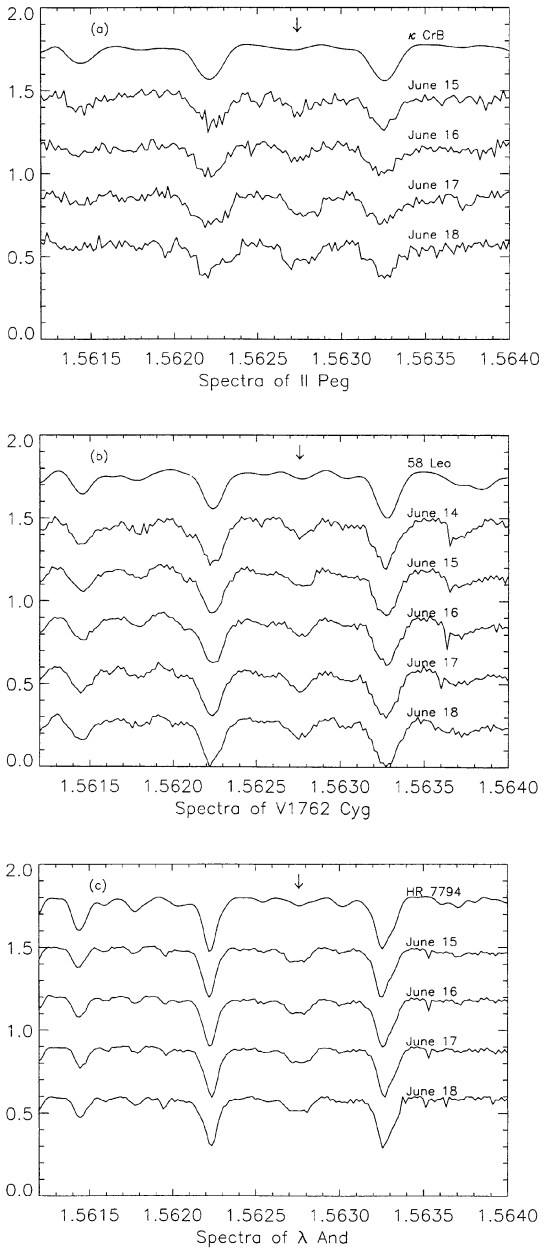

FIG. 4. 1.563 μm spectra of the 3 active stars observed for this program: (a) II Peg, (b) V1762 Cyg, and (c) λ And. The spectra of each active star are compared with an artificially rotationally-broadened spectrum of an inactive comparison star (top) of similar spectral type and $T_{\rm eff}$. Excess absorption in the active star spectra due to starspots is readily seen at 1.5628 μm, marked by arrows.

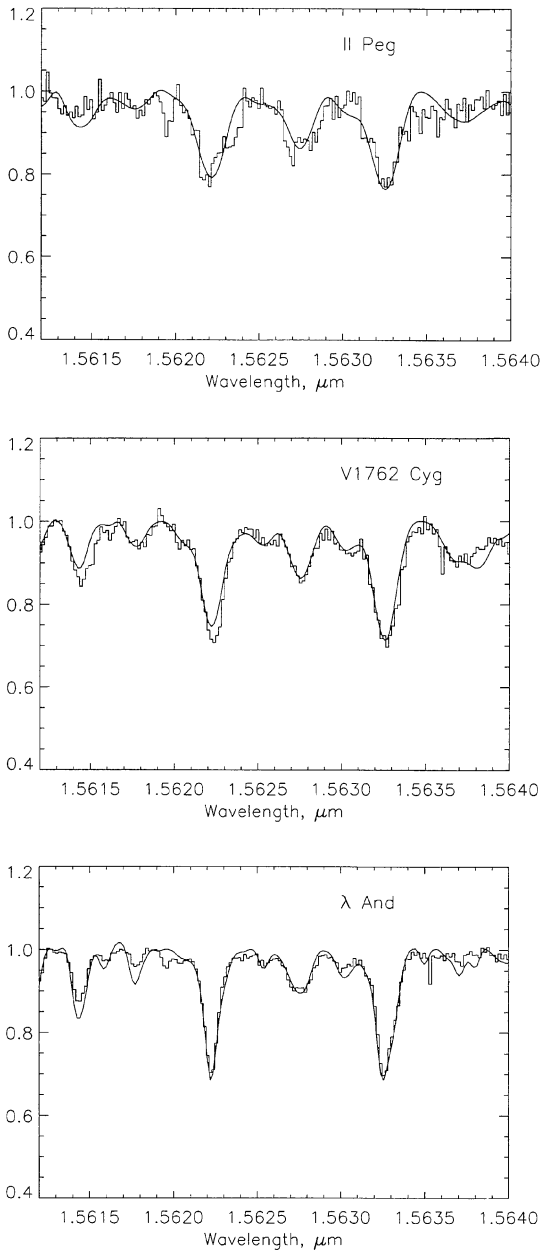

FIG. 5. Best fits computed by STARMOD to spectra of the active stars observed in this program. (a) Fit (solid line) to the June 18 spectrum of II Peg (histogram), assuming $T_{\rm Q}$ = 4800 K and $T_{\rm S}$ = 3550 K. This fit has $f_{\rm S}$ = 0.48. (b) Fit (solid line) to the June 17 spectrum of V1762 Cyg (histogram), assuming $T_{\rm Q}$ = 4600 K and $T_{\rm S}$ = 3475 K. This fit has $f_{\rm S}$ = 0.30. (c) Fit (solid line) to the June 16 spectrum of λ And (histogram), assuming $T_{\rm Q}$ = 4775 K and $T_{\rm S}$ = 3650 K. This fit has $f_{\rm S}$ = 0.21.

crease in R_λ as the cooler spots contribute less light to the overall stellar spectrum.

The companion of II Peg has never been detected; it is probably a white dwarf or an M dwarf. The former would be undetectable in the H-band, and in Paper II we demonstrate that the latter would produce only a very minor effect in the TiO bands. Since an M dwarf companion would be brighter, relative to the primary, in the H-band than in the visible, we explore here the possibility of detecting it through our OH line observations. Vogt (1981) gives $R = 2.2R_\odot$ for the primary, and Gray (1988) gives $R = 0.54R_\odot$ for an M0 V star. $R_\lambda \approx 0.6$ for the temperatures and gravities appropriate to these stars. Assuming that starspots cover 40% of the primary, the unspotted portion of the primary contributes 16.6 times more light at 1.563 μm than the secondary, and the spots on the primary contribute 6.6 times more than the secondary. We model the contribution of this hypothetical sec-

TABLE 4. Measured starspot filling factors.

Star	Date	Phase	f_S
V1762 Cyg	1996 June 14	0.77	0.27±0.06
	1996 June 15	0.80	0.27±0.07
	1996 June 16	0.83	0.29±0.07
	1996 June 17	0.87	0.32±0.06
	1996 June 18	0.90	0.27±0.05
λ And	1996 June 15	0.01	0.22±0.05
	1996 June 16	0.03	0.25±0.05
	1996 June 17	0.05	0.25±0.07
	1996 June 18	0.07	0.26±0.07
II Peg	1996 June 15	0.20	0.37±0.06
	1996 June 16	0.35	0.35±0.05
	1996 June 17	0.50	0.48±0.04
	1996 June 18	0.65	0.45±0.05

ondary with a spectrum of Gl 488 (M0.5 V; $T_{\rm eff}$ = 3700 K) broadened to $v \sin i$ = 5.6 km s^{-1}, the velocity that the M dwarf would have if it is rotating synchronously with the orbital period. Adding the three proxy spectra together with these ratios, we find that the core of the OH line from the system would be only 0.005 deeper (normalized) than if the M dwarf were not present. This would require S/N≳200 to separate from the noise, compared to S/N≈50 achieved in our II Peg spectra. The companion would have to contribute ~17% of the flux for us to detect an M dwarf secondary star in our spectra.

3.2 *V1762 Cygni = HR 7275 = HD 179094*

This RS CVn binary, recently discovered to be an SB2 (Osten & Saar 1997; the secondary is probably G8 V, giving a flux ratio of ~35:1 at 1.56 μm), has a K1 III-IV primary. In Paper 2, we derived T_Q = 4550 K, T_S = 3450±150 K, and f_S = 0.24 in one observation. The star has a 28.6 day period, so our five nights of observation (June 14–18) did not cover a large fraction of a rotational cycle. Weather conditions permitted us to obtain only one pair of spectra of this star on June 14; on the remaining nights we obtained either two or three pairs, which were then averaged to obtain a resultant spectrum for that night.

As for II Peg, we fitted the spectra of V1762 Cyg with 4–6 spot comparison stars and a similar number of non-spot comparison stars having temperatures near to the suspected T_S and T_Q for the active star. The f_S values listed in Table 4 are interpolated for T_S = 3450 K. In Fig. 5(b) we show the best fit to the June 17 spectrum of V1762 Cyg using T_S =3475 K and T_Q = 4600 K; this fit has f_S = 0.30 and an rms residual of 0.024.

3.3 λ *Andromedae = HR 8961 = HD 222107*

The second brightest RS CVn system (after Capella), λ And is a non-synchronous rotator, with $P_{\rm rot}$ = 54.05 d but $P_{\rm orb}$ = 20.5 d. The visible component of this single-lined binary is a G8 III-IV star with $T_{\rm eff}$ = 4750 ±30 K, $v \sin i$ =6.5 km s^{-1}, and log g = 2.5 (Donati *et al.* 1995). The star is active in x-rays (Walter *et al.* 1980; Dempsey *et al.* 1993) and radio (Drake *et al.* 1989), and is a UV flare star (Baliunas *et al.* 1984). O'Neal (1997) derives T_S = 3650±150 K, and f_S between 0.14 and 0.23.

This star is bright enough (V=3.8, H≈1.8) that we needed to take only one pair of observations per night to obtain a high-S/N spectrum. In Table 4 we list the f_S values for λ And obtained from fitting the OH lines using a variety of spot and non-spot comparison stars with temperatures near the presumed T_S and T_Q of λ And. In this case, as assumed T_S rises above 3700 K, the computed f_S also rises when warmer spot comparison stars are used for the fits. Unlike for II Peg and V1762 Cyg, the T_S error bar is the major contributor to the f_S uncertainty for λ And.

In Fig. 5(c) we show the fit to the June 16 λ And spectrum using T_S = 3650 K and T_Q = 4775 K; this fit has f_S =0.21 and an rms residual of 0.023.

4. DISCUSSION

Unlike our TiO-band technique detailed in Papers 1, 2, and 3, this technique only uses one spectral feature and thus cannot place independent constraints on starspot area and temperature. One must assume a T_S, or derive it using another technique such as photometry, before f_S can be calculated.

There are, however, advantages to be gained from observing starspots in OH absorption lines. First, R_λ is much greater in this spectral region than in the visible, so starspots have a greater effect in the overall spectrum. Lower f_S values could be measured using the OH lines, and uncertainties will be less. Also, unlike with the TiO method, starspots warmer than 4000 K will be detectable in OH. Spots in this temperature range have been found for some active stars, including HD 32918 (Piskunov *et al.* 1990). If we assume that the absorption equivalent width of a feature in an active star spectrum is a linear combination of the equivalent widths in the spot and non-spot components (weighted by f_S and R_λ), we calculate that an active star with T_Q = 4800 K, f_S = 0.32, and T_S = 4400 K would have an absorption equivalent width of 0.1 Å for the OH lines studied here. An unspotted star of the same $T_{\rm eff}$ would have an equivalent width of 0.06 Å for the OH features, a difference easily measurable in high-S/N spectra.

5. SUMMARY

We have analyzed spectra of the late-type magnetically active stars II Pegasi, V1762 Cygni, and λ Andromedae showing the 6397 cm^{-1} (1.563 μm 3–1 P2e and P2f [J=5.5]) transitions of the OH molecule. In spectra of inactive stars, the equivalent width of these OH lines increases monotonically as $T_{\rm eff}$ decreases from 5000 K to 3000 K. We clearly see excess OH absorption in the active star spectra compared to rotationally-broadened spectra of inactive comparison stars of the same $T_{\rm eff}$. This is the first detection of OH in starspots. With T_S taken from previous analyses, we find f_S varying from 0.35 to 0.48 for II Peg, 0.27 to 0.32 for V1762 Cyg, and 0.22 to 0.26 for λ And over a 5-night period

in 1996 June. This technique greatly increases the range of starspot temperatures that can be studied via molecular absorption features.

We thank Larry Ramsey for suggesting the original idea to pursue this study, and Steve Saar for insightful comments on an early version of the manuscript. We thank Dick Joyce and Ken Hinkle for their assistance with the NICMASS at the Coudé Feed, and Mike Skrutskie for advice relating to the system he designed. This work was supported by NASA grant NGT-51406 to The Pennsylvania State University from the Graduate Student Researchers Program. This research made use of the SIMBAD database, operated at CDS, Strasbourg, France.

REFERENCES

Ayres, T. R., & Testerman, L. 1981, ApJ, 245, 1124
Baliunas, S. L., Guinan, E. F., & Dupree, A. K. 1984, ApJ, 282, 733
Barden, S. C. 1985, ApJ, 295, 162
Basri, G., & Marcy, G. W. 1983, ApJ, 431, 844
Boyd, L. J., *et al.* 1983, Ap&SS, 90, 197
Byrne, P. B., *et al.* 1995, A&A, 299, 115
Dempsey, R. C., Linsky, J. L., Fleming, T. A., & Schmitt, J. H. M. M. 1993, ApJS, 86, 599
Donati, J.-F., Henry, G. W., & Hall, D. S. 1995, A&A, 293, 107
Doyle, J. G., Butler, C. J., Morrison, L. V., & Gibbs, P. 1988, A&A, 192, 275
Drake, S., Simon, T., & Linsky, J. L. 1989, ApJS, 71, 905
Gray, D. F. 1988, Lectures on Spectral Line Analysis: F, G, and K Stars (Arva, Ontario)
Grevesse, N., Sauval, A. J., & van Dishoeck, E. F. 1984, A&A, 141, 10
Henry, G. W., Eaton, J. A., Hamer, J., & Hall, D. S. 1995, ApJS, 97, 513
Hinkle, K., Wallace, L., & Livingston, W. 1995, Infrared Atlas of the Arcturus Spectrum, 0.9-5.3 microns (ASP, San Francisco)
Hoffleit, D., & Jaschek, C. 1982, The Bright Star Catalogue, 4th ed. (Yale University Obs., New Haven)
Kleinmann, S. G., & Hall, D. N. B. 1986, ApJS, 62, 501
Kürster, M. 1993, A&A, 274, 851
Kurucz, R. L. 1992, RMxA&A, 23, 45
Lançon, A., & Rocca-Volmerange, B. 1992, A&AS, 96, 851
Leroy, J. L. 1962, Ann. d'Astrophys., 25, 127
Neff, J. E., O'Neal, D., & Saar, S. H. 1995, ApJ, 452, 879 (Paper I)
O'Neal, D. 1997, Ph. D. thesis, The Pennsylvania State University
O'Neal, D., Saar, S. H., & Neff, J. E. 1996, ApJ, 463, 766 (Paper II)
Osten, R. A., & Saar, S. H. 1997, MNRAS (in press)
Piskunov, N. E., Tuominen, I., & Vilhu, O. 1990, A&A, 230, 363
Stauffer, J. R., & Hartmann, L. W. 1986, ApJS, 61, 531
Strassmeier, K. G., Hall, D. S., & Henry, G. W. 1994, A&A, 282, 535
Terndrup, D. M., Frogel, J. A., & Whitford, A. E. 1991, ApJ, 378, 742
Tinney, C. G., Mould, J. R., & Reid, I. N. 1993, AJ, 105, 1045
Vogt, S. S. 1981, ApJ, 247, 975
Vogt, S. S., Penrod, G. D., & Hatzes, A. P. 1987, ApJ, 321, 496
Wallace, L., & Livingston, W. 1991, An Atlas of the Solar Spectrum in the Infrared from 1850 to 9000 cm^{-1} (1.1 to 5.4 microns), N. S. O. Technical Report #91-001 (N. S. O., Tucson)
Wallace, L., & Livingston, W. 1992, An Atlas of a Dark Sunspot Umbral Spectrum from 1970 to 8640 cm^{-1} (1.16 to 5.1 microns), N. S. O. Technical Report #92-001 (N. S. O., Tucson)
Walter, F. M., Cash, W., Charles, P. A., & Bowyer, C. S. 1980, ApJ, 236, 212
Wamstecker, W. 1981, A&A, 97, 329
Welty, A. D., & Wade, R. A. 1995, AJ, 109, 326